Global J. Environ. Sci. Manage. 6(1): 15-30, Winter 2020

Global Journal of Environmental Science and Management
(GJESM)

Homepage: https://www.gjesm.net/

ORIGINAL RESEARCH PAPER

Conventional steam activation for conversion of oil palm kernel shell biomass into activated carbon via biochar product

A.C. Affam

[1]*Department for Management of Science and Technology Development, Ton Duc Thang University, Ho Chi Minh City, Vietnam*
[2]*Faculty of Environment and Labour Safety, Ton Duc Thang University, Ho Chi Minh City, Vietnam*

ARTICLE INFO

Article History:
Received 26 April 2019
Revised 20 August 2019
Accepted 20 September 2019

Keywords:
Central composite design
Conventional heating
Oil palm kernel shell
Response surface methodology
Steam activation

ABSTRACT

Conventional steam activation pyrolysis of waste materials such as oil palm kernel shell for production of biochar was investigated using central composite design. Conventional steam activation was carried out via an initial carbonization of oil palm kernel shell to obtain biochar and thereafter steam activation of the biochar using the conventional heating to produce activated carbon. Additionally, removal of chemical oxygen demand and colour was studied alongside the production. Optimum yield was obtained at about 90 min and 725°C. Out of the time duration, 80 min was for carbonation and 10 min was for steam activation. Further extension of time was not significant whereas increasing temperature was able to increase the pores found on the biochar. Under the optimum condition, fixed carbon was 19.39%, chemical oxygen demand and colour removal were 32.02 and 61.15%, respectively at 90 min adsorption time. However, when time was extended to 120 min, chemical oxygen demand (48.2%) and colour (94.19%) removal were achieved. The Brunauer–Emmett–Teller surface area and micropore area of the oil palm kernel shell based activated carbon was 620.45 m^2/g and 550.4 m^2/g, respectively. The conventional steam activation is an effective method that can be employed in production of activated carbon from waste oil palm kernel shell.

DOI: 10.22034/gjesm.2020.01.02

NUMBER OF REFERENCES	NUMBER OF FIGURES	NUMBER OF TABLES
37	9	4

*Corresponding Author:
Email: *augustine.chioma.affam@tdtu.edu.vn*
Phone: +84 28 3775 5035
Fax: +84 28 3775 5035

Note: Discussion period for this manuscript open until April 1, 2020 on GJESM website at the "Show Article.

INTRODUCTION

Palm oil industry generated waste include oil palm trunks (OPT), empty fruit bunches (EFB), palm fronds, palm pressed fibres (PPF) and oil palm kernel shells (OPKS). In the South Eastern Asia, particularly Malaysia, the oil palm kernel shells (OPKS) wasted are up to 4,506 kilotons/year during palm oil production process (Goh *et al.,* 2010). This is an abundant biomass generated annually from the oil palm industry (Loh, 2017). Due to industrialization and scarcity of resources, the need for activated carbon is also on the increase. However, its production process is required to comply with environmental regulation (Lladó, *et al.,* 2016). The activated carbon derived from oil palm kernel shell has adsorption properties that enables it to play an important role in water and wastewater treatment. In addition, the amount of waste generate from palm oil industries would not be an issue to meet this demand (Lladó *et al.,* 2016). The current disposal of OPKS biomass waste by the industry players makes it easy to obtain OPKS from within nearby communities. Recently, the cost of hardwood in the timber industry has become increasingly expensive amidst the fact that resources are limited. New plantations are not easily developed to replace natural forests (Loh, 2017). Hence, the waste from palm oil industry such as OPKS is a veritable replacement material for the hardwood to produce activated carbon. In addition, usage of OPKS for activated carbon production is an environmental friendly approach and an ideal solution that could be adopted for appropriate waste management practice. The production method of OPKS derived activated carbon is a fundamental factor that could affect the end material in terms of its engineering properties. The two commonly used methods for activated carbon production by carbonization includes conventional and microwave heating (Jamaluddin *et al.,* 2013). The microwave heating method is reported to be more efficient technically and economically compared to the conventional heating. However, the produced amount via microwave method in practical terms would not be sufficient to meet actual demand for activated carbon. More hands are needed and most people worldwide have not adopted the new technology especially in very remote areas or communities. As such the conventional heating still remains largely a method most people are able to handle and can produce large amounts of activated carbon. While microwave pyrolysis may have superb advantages including rapid heating and easy temperature control during the biochar production (Domeño and Nerín, 2003), challenges exist in terms of requiring more time and higher energy consumption rate due to low thermal conductivity of biomass waste materials (Haeldermans *et al.,* 2018). The prolonged duration usually promotes some undesired secondary reactions which would likely cause other pyrolysis-volatile related toxic compound formation (Makul *et al.,* 2014). In addition, poor heating heterogeneity especially in cases where the material is not hard or tough enough could lead to the need for salts such as potassium carbonate (K_2CO_3 or KOH) addition to microwave absorber materials including commercial activated carbon in order to allow homogenous heating in the microwave oven (Foo and Hameed, 2012). Another study observed that the total and fixed carbon content were significantly lower in microwave produced biochar compared to that obtained from the conventional heating process (Haeldermans *et al.,* 2018). The conventional heating would still be around for a long time to come especially with new technologies such as the double insulated carbonization-activation reactor (Zainal *et al.,* 2018) which was recently patented, and to be made available in no distant time. The issues of trapping gaseous materials, particles and fumes that could be harmful during the production phase of activated carbon via OPKS or other materials from palm oil industry would be minimum. In addition, improvement of textural characteristics, surface area, and combination of carbonization and activation phase in one chamber would lead to an overall reduction in the cost of production (Zainal *et al.,* 2018). Although some studies have reported the production of OPKS via conventional process (Thiagarajan *et al.,* 2018; Wai *et al.,* 2017), they have reported use of one-variable-at-a-time (OVAT). Process optimization remains sparsely reported and also challenging and this creates a window for more studies to be undertaken. The novelty of this study was combining central composite design (CCD) to minimize the number of experiments required to be carried out using a one-step conventional steam activation approach to produce activated carbon via biochar from OPKS. This study attempts to bridge the gap in literature as the use of one-variable-at-a-time (OVAT) method can be time, material and cost

involving (Jacynal *et al.,* 2019). This study was carried out in East Malaysia during the dry season of 2018. This work provides alternative ways of waste disposal and reduction of unwanted environmental hazards as against excessive biomass burning and haze effect experienced frequently in this region.

MATERIALS AND METHODS

Materials

The raw oil palm kernel shell (OPKS) was obtained from a local palm oil mill. The methylene blue dye was purchased from a local shop and used as obtained. A conventional oven was used for production of the activated carbon. Temperature ranged from 0 to 1100°C. Steel pipe was fabricated to house the biochar production chamber inside the oven.

Wastewater

The dye wastewater was simulated in the laboratory. Methylene blue ($C16H18N_3SCl.{}_3H_2O$) was used as the model pollutant in this experiment. The dye concentration was prepared by dissolving 5 mg of dye in 1 L distilled water (Pathaniae *et al.,* 2017).

Batch production studies

Batch production of the biochar via conventional heating followed the designed CCD using the RSM tool. Steam was transferred when needed through a connected chamber to provide sufficient activation at a temperature of 600°C in a limited time duration of 10 min. A generator producing steam at 0.2 MPa maximum pressure was employed in this phase. The steam flow rate was at 5 g/min and this was chosen to carry out the activation. This was because it could be detrimental to the system if higher rate was selected (Xin-hui *et al.,* 2011).

Analytical methods

Determination of COD and colour was according to Standard Methods for examination of water and wastewater (APHA, 2005).

Assumption of input parameter during adsorption

In other to carry out the adsorption tests and measure COD and colour removal, assumptions taken were according to the work by Pathania *et al.* (2017). These includes, orbital shaking speed = 200 rpm, contact time = 60 min, methyl blue dye concentration = 50 mg/L, pH value = 8 and adsorbent dose = 5 g/L. This was a preliminary test to know the performance of the produced activated carbon in terms of colour and COD removal from dye wastewater.

Material Synthesis Characterization

The synthesized activated carbon via OPKS biochar was characterized before and after production in a number of ways as explained in the subsection below.

Fourier transform infrared spectroscopy

The activated carbon via OPKS biochar surface chemistry was analyzed using Fourier transform infrared spectroscopy. This was done by identification of functional groups and/or bonds of the organic compounds present in the material. FTIR-2000, Perkin Elmer was used to record the spectra ranging from about 4,000 to 400/cm.

Scanning Electron Microscope

Scanning electron microscope (SEM) test was carried out using a scanning electron microscopy, Joel brand (JSM-7900F Schottky Field Emission Scanning Electron Microscope). This generated the detail and signals from the sample solid surface. The raw sample and produced activated carbon were placed on a disc and held in place using a double-sided carbon tape. Then it was coated with gold particles to avoid sample charging. Thereafter, the image was generated.

Proximate analysis

The proximate analysis of the oil palm kernel shell (OPKS) was carried out according to the standard methods (ASTM D 3174, E-870-06) in order to obtain the moisture content, volatile matter, fixed carbon, and ash content as required.

BET and pore size area

The Brunauer–Emmett–Teller surface area and micropore area, were measured by Brunauer–Emmett–Teller (BET) surface area apparatus (ASAP 2000, Micrometrics) at 77°K by means of standard BET procedure using N2 adsorption. Prior to the measurement, the samples were degassed at 120°C for 3 h.

Experimental design matrix and range of input parameters

The central composite design (CCD) is very widely employed in experimental design in order to

ensure sequential testing of lack-of-fit by applying considerable number of design points. In addition, it helps to ensure statistical analysis of the effect of the input variables on the chosen response. The appropriate variable ranges were obtained from preliminary experiment and with reference to prior studies. The range of input variables for the CCD were 500 to 900°C for temperature and 60 to 120 min time duration. These were the low and high ranges preset in the software to generate the set of experiments. During the study, a maximum number of 13 experiments were designed according to the CCD for assessment of the random error (Behera *et al.,* 2018). The optimum operating variables were identified from the response surface plots and the response equation simultaneously, using Eq. (1).

$$Y = \beta_o + \beta_1 A + \beta_2 B + \beta_{11} A^2 + \beta_{22} B^2 + \beta_{12} AB \quad (1)$$

This was used to assess the predicted result (Y) as a function of the variables. Temperature (A), and reaction time (B), and estimated as the sum of a constant (βo), two first-order effects (A and B), two second-order effects (A^2 and B^2) and one interaction effect (AB). The response surface methodology (RSM) was adopted to investigate the optimal conditions that would maximize biochar production process. The experiment was designed so as to minimize the required operational input factors such as reaction time and temperature in order to maximize yield. To assess the performance of the produced biochar, dye wastewater was treated, and chemical oxygen demand (COD) and colour removal were measured.

Adsorption isotherm models

The equilibrium adsorption isotherms are most important to understand the mechanism of an adsorption system. Langmuir and Freundlich isotherms represents the equilibrium distribution of ions between the solid and liquid phases, defining the correlation with the amount of adsorption and liquid phase concentration. The Langmuir isotherm is based on the assumption that the adsorption will take place only at specific localized sites on the surface and the saturation coverage corresponds to complete occupancy of these sites; each site can accommodate only one molecule and the surface is energetically homogeneous (Chen, 2015). The adsorption isotherm for heterogeneous surface is fully described by the Freundlich adsorption isotherm, whose main assumption is that the ions can be applied for multilayer sorption (Chen, 2015). The linear and non-linear isotherm model equations are given in Eqs. 2 to 5.

Langmuir nonlinear equation, $q_e = (Qb\,C_e)/(1 + b\,C_e)$ (2)

Langmuir linear equation, $C_e/q_e = 1/Qb + C_e/Q$ (3)

Freundlich nonlinear equation, $q_e = K_f C_e^{1/n}$ (4)

Freundlich linear equation, $log\ q_e = log\ K_f + 1/n\ log\ C_e$ (5)

Where

q (mg/gm) = Maximum amount of adsorption with monolayer

b (L/mg) = Langmuir constant

K_f (mg/g) (L/mg)/n and 1/n = Heterogeneity factor related to Freundlich constants.

a and b = slope and intercept and can be obtained from linear plots of C_e/q_e versus C_e, respectively.

K_f and 1/n can be estimated from intercept and slope of the linear plot between log C_e against $log\ q_e$, respectively.

RESULTS AND DISCUSSION

Proximate analysis of the palm kernel shell, biochar and activated carbon

The results obtained appear consistent with other studies with an improvement in the fixed carbon content most importantly. The low content of ash in OPKS suggests that the OPKS can be used as raw material in the production of activated carbon and it would be effective for adsorption of pollutants. In addition, low ash content would produce a relatively low content of inorganic component in the eventual activated carbon. The moisture, ash content, volatile organic matter, and fixed carbon of the OPKS biochar based activated carbon was 7.0, 1.34, 72.27 and 19.39%, respectively. Brunauer–Emmett–Teller surface area and micropore area of the oil palm kernel shell based activated carbon was 620.45 m^2/g and 550.4 m^2/g, respectively. This could be compared to commercially available activated carbon whose area is around 690.92 m^2/g and micropore area of 469.08 m^2/g (Rugayah *et al.,* 2014). The nature and distribution of lignin, hemicellulose, and cellulose in the base material such as OPKS is responsible for

increased fixed carbon content. Increase in lignin and minerals content would normally lead to a high biochar yield (Chang *et al.,* 2018). Table 1 compares the characteristics of the raw OPKS, biochar and eventual activated carbon along with recent studies conducted. It was found that the fixed carbon in this study was more than in the other reports. This is a fundamental characteristics required to identify a good activated carbon adsorbent produced from waste materials. Thus the most significant in comparison with other studies. The moisture, ash content, volatile organic matter, and fixed carbon of the OPKS biochar based activated carbon was 7.0, 1.34, 72.27 and 19.39%, respectively. The grade of activated carbon was similar to commercially available products. The Brunauer–Emmett–Teller (BET) surface area and micropore area of the oil palm kernel shell based activated carbon was 620.45 m^2/g and 550.4 m^2/g, respectively. This could be compared to commercially available activated carbon whose area is around 690.92 m^2/g and micropore area of 469.08 m^2/g (Rugayah et *al.,* 2014). The nature and distribution of lignin, hemicellulose, and cellulose in the base material such as OPKS is responsible for

Table 1: Properties of raw OPKS, biochar and activated carbon and comparison with previous study (1* Chan *et al.,* 2018; 2* Rueda-Ordóñe *et al.,* 2019)

Present element	This study OPKS	Biochar	Activated carbon	Previous studies	
				1*	2*
C	51	60	72	50.3	45.78
H	7	4	2	6.05	5.86
N	3	1	0.4	0.46	-
S	0	0	0	0	-
O*	39	35	25.6	43.18	43.95
Proximate content	This study	1*	2*		
Moisture content	7	0	6.28		
Volatile organic matter	72.27	80.7	85.38		
Fixed carbon	19.39	14.68	10.88		
Ash content	1.34	4.61	3.74		
BET Surface area (m^2/g)	620.45	-	-		
Micropore area (m^2/g)	550.4	-	-		

O* calculated by difference

Table 2: The results of experimental matrix design

Stand	run	Time, (min)	Temp. (°C)	Yield (%)		Colour removal (%)		COD removal (%)	
				Predicted value	Actual value	Predicted value	Actual value	Predicted value	Actual value
1	1	60	500	34.00	34.70	22.00	19.22	16.00	15.86
5	2	47.57	725	34.00	32.10	35.00	22.85	14.00	10.96
13	3	90	725	24.00	24.15	64.00	63.90	33.00	33.54
3	4	60	950	25.00	23.55	94.00	95.53	48.00	45.64
10	5	90	725	28.00	27.45	29.00	30.77	22.00	21.20
9	6	90	725	27.00	27.30	64.00	63.48	23.00	26.30
4	7	120	950	39.00	37.48	19.00	21.52	9.00	7.51
11	8	90	725	24.00	22.27	98.00	96.73	47.00	47.77
8	9	90	1043.2	29.00	27.60	40.00	41.40	27.00	24.60
6	10	132.43	725	28.00	27.60	40.00	41.40	32.00	24.60
2	11	120	500	28.00	27.60	49.00	41.40	27.00	24.60
12	12	90	725	27.00	27.60	36.00	41.40	17.00	24.60
7	13	90	406	26.00	27.60	42.00	41.40	20.00	24.60

increased fixed carbon content. Increase in lignin and minerals content would normally lead to a high biochar yield (Chang *et al.,* 2018). The findings were comparatively at par better with the studies conducted by Chan *et al.* (2018); Ahmad *et al.* (2019) and Rueda-Ordóñe *et al.* (2019) as shown in Table 1.

Central composite design

The yield (%) of biochar, pollutant removal efficiencies (%) in terms of COD and colour were tested in duplicates. The response obtained was statistically evaluated to determine the model significance. The experimental design of the input variables (predicted and actual), and corresponding responses are shown in Table 2.

Textural, size and surface characterization

The scanning electron microscope (SEM) image of the OPKS before and after conversion into biochar is shown in Fig. 1a and b. There is a large activated adsorption site i.e. surface area created as seen in the SEM of the biochar produced after the conventional heating process of OPKS. The BET surface area and microspore area of the OPKS based activated carbon was 620.45 m^2/g and 550.4 m^2/g, respectively. From Fig. 1a and 1b, it can be seen that after conventional heating process, the organic components of the OPKS were liberated, thereby forming well-developed pore space in between the structure and showing the pore structure (Foo and Hameed, 2012).

FTIR analysis

In the Fourier transform infrared (FTIR) spectroscopy, a tiny proportion of photons incident on the raw OPKS and the activated carbon causes vibrations such that there is an eventual scattering

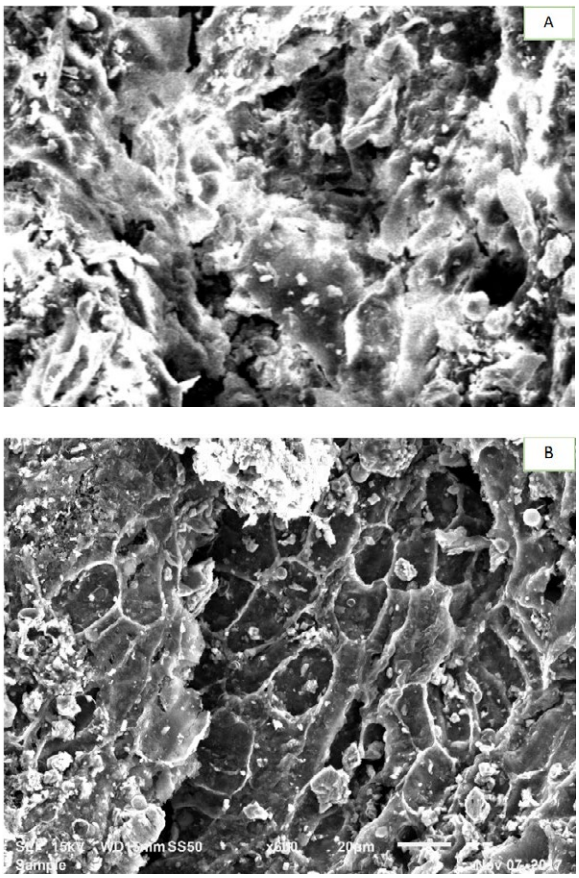

Fig. 1: The SEM of (A) before and (B) after the biochar was produced from OPKS

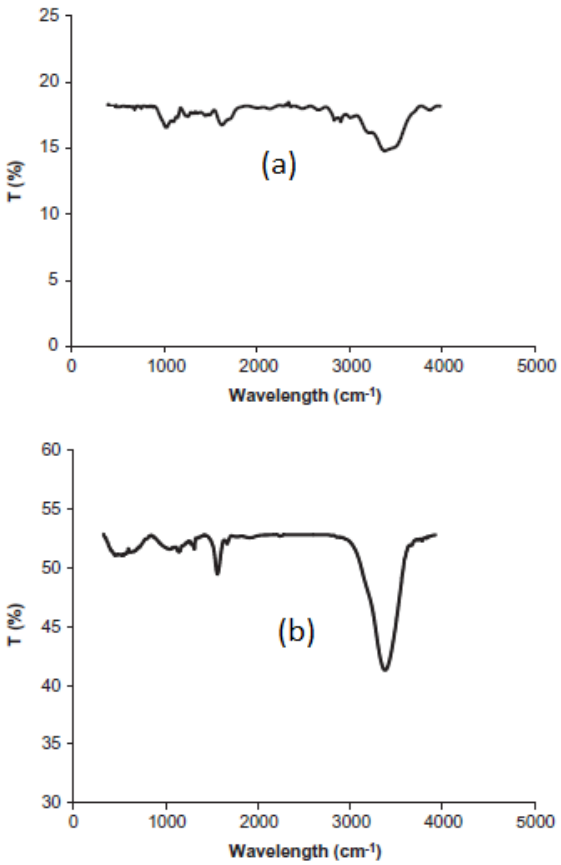

Fig. 2. The FTIR spectra of (a) before, and (b) after, conversion of OPKS into activated carbon

of light at higher or lower energy to represent the spectra. The FTIR spectra before and after production of the biochar based activated carbon can be seen in Fig. 2. Before production of the biochar, the designated band of O-H stretch contains OH, alcohols and phenols was observed between the bands 3500–3300 cm^{-1} and was confirmed in another study (Sumathi *et al.,* 2010). In the sample before and after production, the bands between 2300 –2400/cm represent the functional group –COOH. The bands found between 1600 and 1400/cm indicate the presence of the C=C stretch of aromatics. It is obviously seen on both samples. This means that both have same functional groups and can be identifiable. The carbonyl C-O stretch around 1600 and 1400/cm band were further modified during the production process as can be seen in Fig. 2. In addition, the bands seen around 1740 and 1710/cm which represents C=O band stretch containing saturated aliphatic, aldehydes in the raw OPKS was modified after activation and biochar production. This was as a result of the instability of the ketonic and aldehyde groups at considerably high temperatures (Guo and Lua, 2002). Vibrations which occur in ethers and associated with C-O stretch band was seen in the OPKS before conversion. It was modified and eventually unseen after biochar production. This was due to the high temperature sample was subjected to leading to destruction of C-O and C=O functional groups (Guo and Lua, 2000) and formation of poly aromatic structures (Abdul Hamid *et al.,* 2014). Activation is reported to also lead to destruction of ester and ether linked groups which support the lignin structures (Abdul Hamid *et al.,* 2014). Increasing temperature also has an additional effect of causing decomposition of cellulose and hemicellulose which fundamentally makes a functional group to be modified or disappear from the spectra. The band between 1300 and 1000/cm stretch shows the ether vibrations. Modification of the band was also observed.

Effect of time and temperature on biochar yield

The effect of production time and temperature on the biochar product in terms of the yield (%) is shown in the contour plot of Fig. 3. It can be seen that the time variable does not fully govern the yield value. As time increased from 60 until about 90 min, the biochar yield (%) decreased and a further increase beyond 90 min increased the yield. This may indicate that full decomposition of the organics including the volatile gases as well (Zhang *et al.,* 2015). There would be no need to

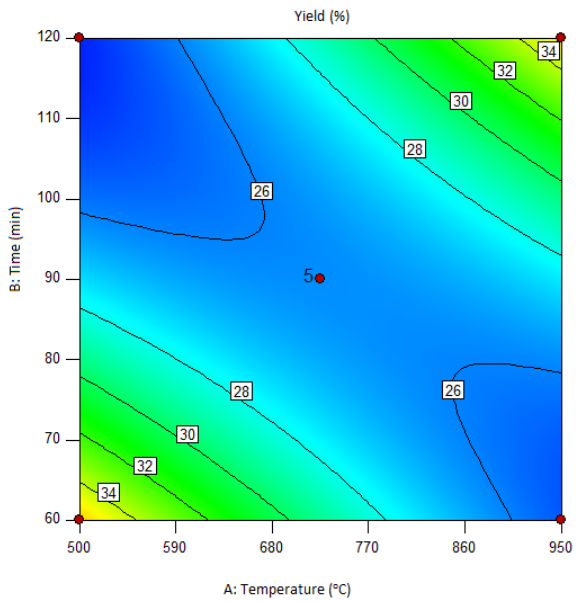

Fig. 3: Time and temperature effects on biochar yield (%)

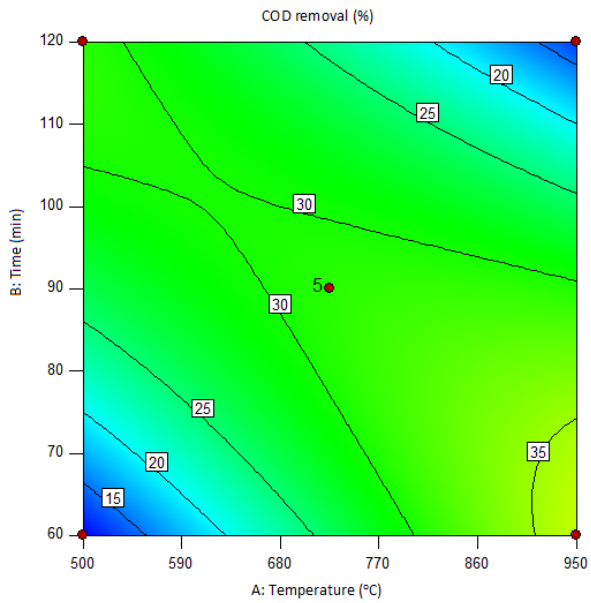

Fig. 4: Time and temperature effect on COD removal (%)

continue increasing the time beyond this point as it may reduce the activated carbon stability when in use and thus limit its performance. A similar study reported that time had a low effect especially when the temperature was low. In our study, increase in temperature required a lower time duration for the biochar production (Fig. 2). An increase in temperature is known to only change the biochar surface area and internal structure whereas its contribution to the biochar yield is less (Junna *et al.,* 2016). Temperature control in the conventional pyrolysis affects the pore formation all over the biochar. As temperature increases, more pore structures are formed due to the liberation of organic matter in the material. Thus making adsorption capacity increase. As temperature increase, volatile gases contained in the biomass are usually released. Thus, the vesicles available on the surface of OPKS would bust after cooling and a good number of pore structures would appear (Zhao *et al.,* 2017). This is evident from the SEM images reported in this work.

Effect of time and temperature on COD removal

The effect of production time and temperature on the biochar product in terms of the COD removal (%) is shown in the contour plot of Fig. 4. It was observed that an increase in time up till 90 min increased COD removal, beyond which the COD decreased significantly. In the same vein, increasing temperature showed an increase in COD. Any further increase in temperature beyond led to a decrease in COD removal. However, spectacular phenomenon was observed when the temperature reached between 900 and 950°C. At this point, a very minimal time (about 60 to 70 min.) was required to obtain high removal of COD. Poor COD removal indicates the organics were recalcitrant and required a further treatment to break down the organic bonds (Amor *et al.,* 2019). It has been reported that increasing temperature beyond a certain point completely destroys the pore structure of the biochar and this should be avoided (Junna *et al.,* 2016). This must have played out when the temperature was increased. It should be noted that temperature was more significant than time in affecting the overall process. In a case where the OPKS usage is targeted for COD removal, minimum time must be used during pyrolysis.

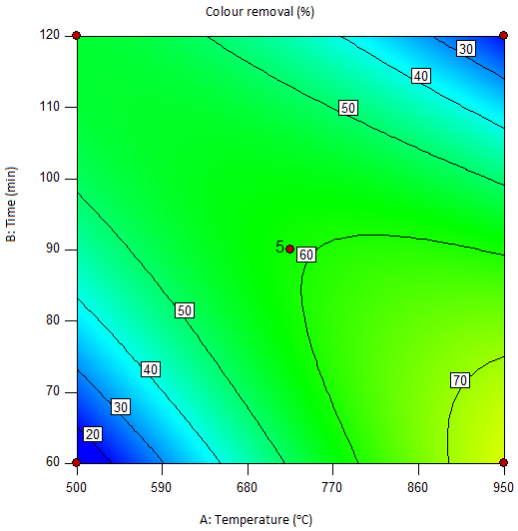

Fig. 5. Time and temperature effects on colour removal (%)

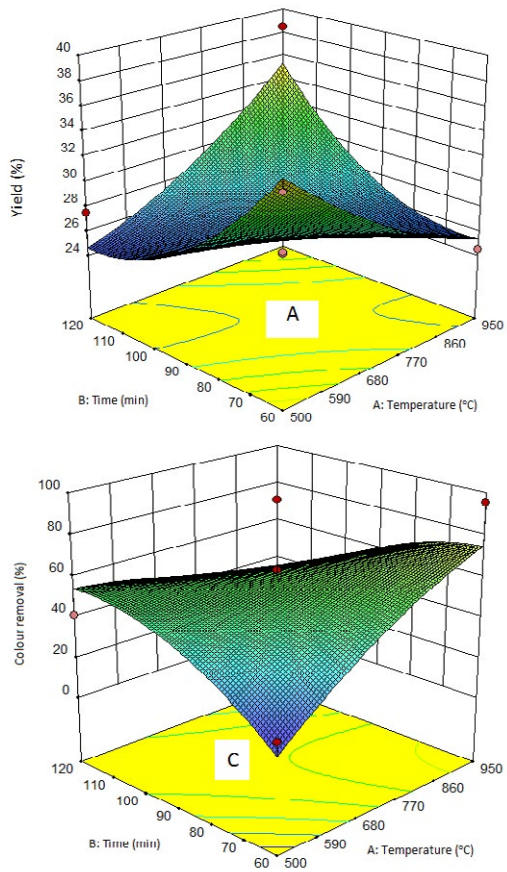

Fig. 6: 3D Plot of (A) biochar yield (%), (B) COD removal (%) and (C) Colour removal (%)

Effect of time and temperature on colour removal

The effect of pyrolysis time and temperature on the biochar product in terms of the colour removal (%) is shown in the contour plot of Fig. 5. An increase in temperature of production led to decrease in the yield (%) whereas an increase in temperature led to increased removal of colour. When the temperature reached at a peak value of 950°C, the colour removal reached the maximum as well. It was observed that increasing time of production of biochar led to a corresponding increase in colour removal. However, beyond 90 min it was observed that colour removal declined (Fig. 5). Similar results have been reported in reviews (Dai *et al.,* 2019). However, when temperature was about 950°C, the colour removal was maximum albeit at a reduced time duration of between 70 and 75 min. of pyrolysis (carbonation and activation).

Process analysis

The performance of the process was statistically analyzed using analysis of variance (ANOVA) in order to confirm the reliability of the RSM diagnostic tools. The selected models for biochar yield (Y_1), COD (Y_2) and colour (Y_3) removals were significant by the *F*-test at 95% level of confidence only when the prob.>F<0.05. The regression equations fitted well to the second-order polynomial (Eqs. 6, 7 and 8) and were used to ascertain the quantitative effects of temperature (A) and time (B) during the pyrolysis in order to predict COD and colour removal (%) expressed as coded factors.

For biochar yield,

$$Y_1 = 26.16 + 0.094A - 0.30B + 5.26AB + 1.25A^2 + 2.87\ B^2 \quad (6)$$

For COD removal,

$$Y_2 = 30.6 + 1.98A - 0.86B - 10.91AB - 2.28A^2 - 5.70\ B^2 \quad (7)$$

For colour removal,

$$Y_3 = 59.25 + 7.03A - 3.20B - 24.05AB - 6.99A^2 - 11.66\ B^2 \quad (8)$$

In Eqs. 2, 3 and 4, the values of sum of constant (βo), 26.16, 30.6 and 59.25 represent biochar yield, COD and colour removal (%), respectively. A positive and negative sign indicates direct proportion and an inverse proportion, respectively, of input factors contributing to the response factor. The plots shown in Fig. 6a and c depicts the 3D

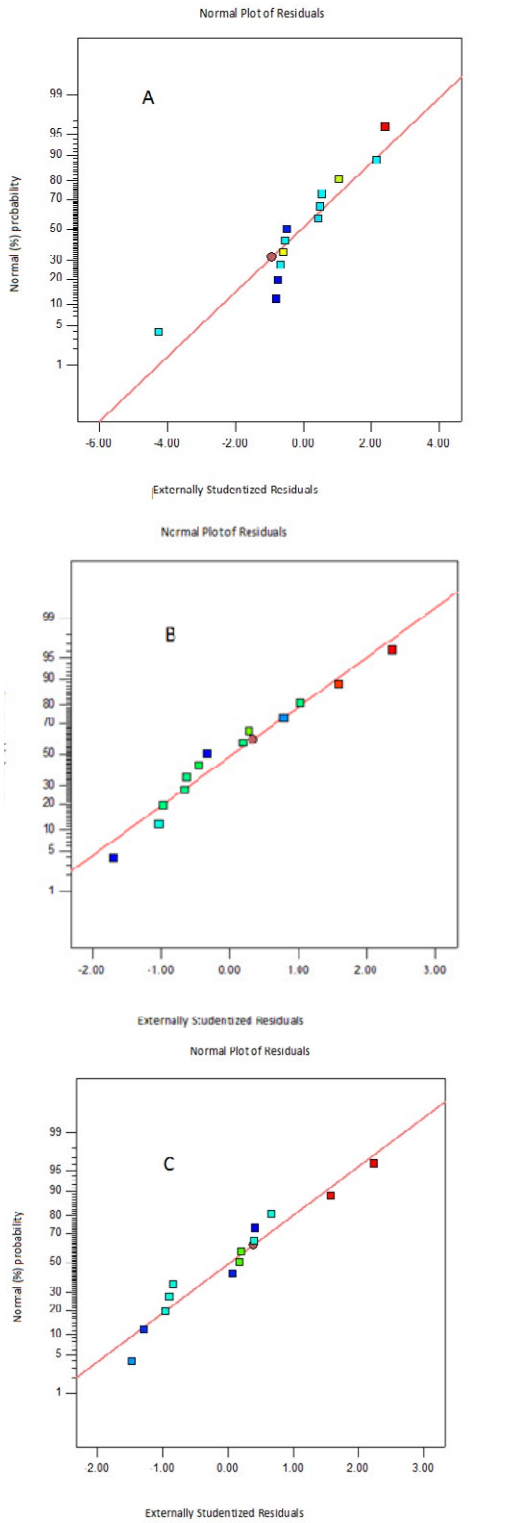

Fig. 7: Normal percentage of probability versus studentized residuals for (a) biochar yield (b) COD removal and (c) colour removal

view of the yield, COD and colour removals. Fig. 6a shows the response surface plot for biochar yield (%). Accordingly, optimized yield was 28.4%. Fig. 6b shows the optimized COD removal was 21.1%. Similarly, Fig. 6c shows that the colour removal was about 35.56%. In all three cases, the optimum values were at about 750°C and reaction time 90 min.

In an attempt to ascertain the variance in the data obtained, a plot of the studentized residual and predicted values (figures not shown) indicated a random arrangement of the points between the boundaries and this confirmed the prediction was satisfactory as all points were within the region as described by quadratic Eqs. 2, 3 and 4. In the normal (%) probability, it indicated that the data obtained were normally distributed as they were along the line of best fit (Fig. 7).

Further to this, the study indicated that all input variables were significant from the perturbation diagnostics plot (figure not shown). When the line has a curvature, the input parameter is deemed a significant contributor to the treatment process. A sharp curvature indicates a better contribution to the process compared to a straight line. All the input factors where of importance during the experimental phase.

Analysis of variance

In order to further ascertain the model accuracy, the data obtained from the experiment were subjected to analysis of variance (ANOVA) to statistically test the model (Table 3a and c). The assessment of the F-value, p-value, sum of squares (SS), mean squares (MS), and degree of freedom (df) were done by the ANOVA (Mazhari *et al.,* 2018). In the biochar yield (%), COD and Colour removal (%), the model had F-value of 5.71%, 5.75%, and 3.19%, respectively. Thus implying that the models were all significant. The p values were 0.0201, 0.0201, and 0.0146. A statistically significant model should have a *p*-value less than or equal to 0.05 with a 95% confidence level. The data which was fitted to the model had a minimal variation with the

Table 3a: Analysis of variance (ANOVA) for biochar yield

Source model	SS	df	MS	F value	p-value Prob. > F
Model	145.60	5	29.12	5.71	0.0205
A-Temperature	46.35	1	46.35	9.09	0.0195
B-Time	0.23	1	0.23	0.045	0.8385
AB	71.32	1	71.32	14.00	0.0073
A^2	6.13	1	6.13	1.20	0.3090
B^2	18.34	1	18.34	3.60	0.0996
Residual	35.67	7	5.10		
Lack of fit	19.18	3	6.39	1.55	0.3322
Pure error	16.49	4	4.12		

Table 3b: Analysis of variance (ANOVA) for COD removal

Source model	SS	df	MS	F value	p-value Prob. > F
Model	1300.60	5	260.12	5.75	0.0201
A-Temperature	144.37	1	144.37	3.19	0.1172
B-Time	0.67	1	0.67	0.015	0.9065
AB	939.42	1	939.42	20.76	0.0026
A^2	16.08	1	16.08	0.36	0.5699
B^2	211.60	1	211.60	4.68	0.0674
Residual	316.77	7	45.25		
Lack of fit	177.23	3	59.08	1.69	0.3050 not significant
Pure error	139.54	4	34.88		

Table 3c: Analysis of variance (ANOVA) for Colour removal

Source model	SS	df	MS	F value	p-value Prob. > F
Model	6416.99	5	1283.40	6.49	0.0146
A-Temperature	*875.15*	*1*	*875.15*	*4.42*	*0.0735*
B-Time	*21.58*	*1*	*21.58*	*0.11*	*0.7509*
AB	*4182.21*	*1*	*4182.21*	*21.14*	*0.0025*
A^2	*349.86*	*1*	*349.86*	*1.77*	*0.2253*
B^2	*1129.41*	*1*	*1129.41*	*5.71*	*0.0482*
Residual	1385.14	7	197.88		
Lack of fit	*1098.34*	*3*	*366.11*	*5.11*	*0.0746 not significant*
Pure error	*286.80*	*4*	*71.70*		

residual error and pure error. In the biochar yield (%), COD and Colour removal (%), the lack of fit was 0.3322, 0.3050, and 0.0746, respectively. The model indicated lack of fit (*PLOF)* value was greater than 0.05 and which was good for the model. Adequate precision measures the ratio of signal to noise effects. An acceptable ratio should be greater than 4. In the biochar yield, COD and colour removal, A.P. was 8.65, 8.57 and 8.96% which indicated that all three models were adequate. The R^2 value was 0.80, 0.80 and 0.82 for biochar yield, COD and Colour removal, processes, respectively. High R^2 value usually indicates the process is efficient (Karimifard *et al.,* 2018). The coefficient of variation (C.V.) indicates the reproducibility of the treatment process. In the three processes, C.V. was 8.05%, 26.36%, 29.45%, respectively. In other to have an assured reproducibility, C.V. should be fairly consistent irrespective of boundaries or location of test (Karimifard *et al.,* 2018).

Optimization and validation of model

In order to validate the three model responses obtained, two confirmatory experiments were conducted under each optimal conditions for biochar yield, COD and colour removal. The model predictions for biochar yield, COD and colour removal were 26.16, 30.6 and 59.25, respectively.

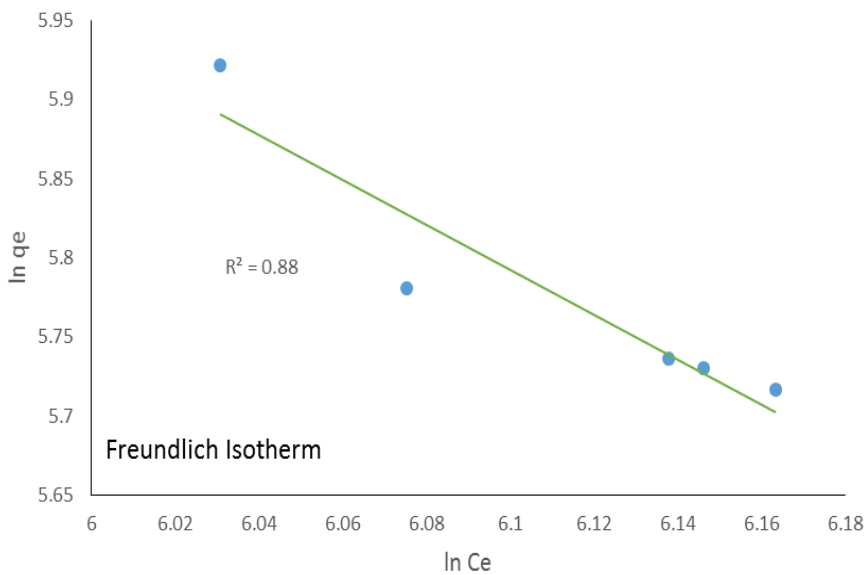

Fig. 8: Freundlich Isotherm for adsorption of Methylene blue OPKS based activated carbon

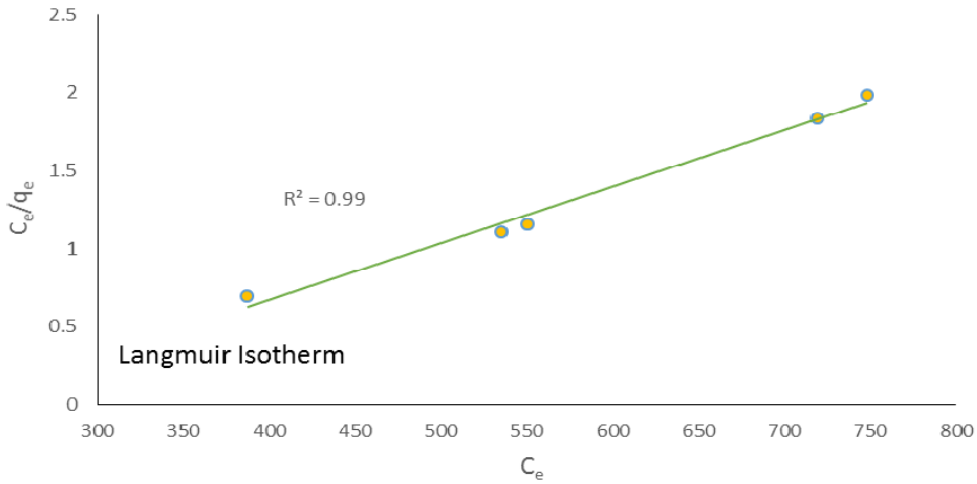

Fig. 9: Langmuir Isotherm for adsorption of Methylene blue by OPKS based activated carbon

Table 4: Costing of produced activated carbon via OPKS biochar

Item	Time (min)	Electricity cost (OPKS)	Commercial AC cost
(a) Oil palm kernel shell purchase	N/A	N/A*	
(b) Carbonization and steam activation of the OPKS	90	RM 0.79 cent per kg	RM 35 per kg
(c) Transportation cost of materials to processing plant		RM 0.25cent per kg	
Total		RM 1.04 USD 0.25	RM 35 USD 8.54
(a) N/A* No purchase cost since it is owned by palm oil mill			

Whereas after duplicate sampling and testing, the confirmatory tests from the experiments, the response were 27.51, 32.02 and 61.15%, respectively. The model prediction and experimental efficiency (actual) data were in a close agreement of less than 5.0% error. This is good for the model developed for all three responses. However, when one factor at a time (OFAT) was performed and time was increased up to 120 min, the COD and colour removal increased from 30.6 and 59.25 to 48.20 and 94.19%, respectively. Since the main target of the process was to obtain a good biochar yield, which was possible, the experimental time for pollutant removal maybe extended. This was implemented to show that the produced AC via OPKS biochar can perform better given more time for treatment purpose.

Adsorption Isotherm model

The performance of activated carbon in adsorbing pollutants can be described through the adsorption isotherm. Isotherm analysis is significant in predicting and comparing the adsorption behavior, understanding the adsorption mechanism, and optimizing the adsorption system (Chen, 2015). From Figs. 8 and 9, it can be seen that the data fitted better to the Langmuir isotherm model (R^2 = 0.99) than the Fruendlich isotherm model (R^2=0.88), which indicates that the pollutant removal process was on the single layer. The intermolecular forces depends on distance and expected that a monolayer coverage exist at the outer surface of the OPKS biochar adsorbent. It can be assumed that the adsorption process will only occur at particular homogeneous sites in the

produced activated carbon and validated by the Langmuir isotherm model.

Cost of production of the OPKS based activated carbon

The cost of production of the OPKS based activated carbon was studied in order to propose it for local needs. Although cost of producing enables proper evaluation of its economic feasibility, it may be needed when change in alternative source of procurement is being planned by companies who rely on activated carbon for a number of their processes. In addition, it could be a fundamental issue in advertising a new product in the market or a unique entry strategy (Ahmed *et al.,* 2016). The entire costing was done considering the cost of palm kernel shell (if any), local transportation and electricity consumed by the conventional heating pyrolysis process (Table 4). These make up the actual operation cost during production. Purchase of oil palm kernel shell comes at little or no cost since it is from the oil palm mill. The cost of electricity currently stands at 39.45 cent KWh. The entire time required for heating was 90 min. Additional cost of RM 25 per kg for transportation was provided in case movement of the waste was necessary. The total cost estimate per kg was obtained by addition of the transport cost and electricity multiplied by the heating time to obtain RM1.04 (USD 0.25) per kg. This is cheaper than that reported by Selvaraju and Baker (2017) which was RM27/kg and in comparison to commercially available stocks which are up to 35 to RM40 (about USD 10) per kg in the local market. Therefore, it is fair to note that the potential of activated carbon via OKPS biochar production is a huge potential and has high feasibility in terms of economics, technology and markets. The commercialization should be easy to implement in the near future.

CONCLUSION

This study shows that waste materials such as oil palm kernel shell are huge potential for replacing wood for the purpose of manufacturing activated carbon. Conventional steam activation pyrolysis under optimum operating conditions (90 min and 725°C) were sufficient to produce activated carbon yield of 19.39% fixed carbon and removed as much as 94% colour and 48% COD from dye wastewater. The ANOVA analysis indicated that the production process of activated carbon via biochar was statistically significant with $p < 0.05$, and significant performance of the biochar fixed carbon content, in terms of COD and colour removal. It was observed that increasing time of experiment would have a marginal effect compared to increase in temperature during production of the biochar. On the other hand, an extreme temperature would decrease the quality of the produced biochar. The input parameters correlated well with the quadratic equation and design space. Developed models were validated by statistical analysis and experimental tests. The cost of production was evaluated and was found reasonable and lower than available commercial activated carbon. This makes it affordable when eventually introduced into the market on a large scale. In subsequent study, investigation of likely toxic gaseous substances that maybe produced in biochar process such as dioxins and polycyclic aromatic hydrocarbons (PAHs), etc. would be studied. These have been sparsely reported in many studies. The procedure adopted in this study is efficient for the purpose of high quality activated carbon via OPKS biochar. In addition, produced biochar is capable of removing COD and colour from dye wastewater.

ACKNOWLEDGEMENT

The author is thankful to the management and authorities of Ton Duc Thang University, Ho Chi Minh City, Vietnam for supporting this study.

CONFLICT OF INTEREST

The author declares that there is no conflict of interests regarding the publication of this manuscript. In addition, the ethical issues, including plagiarism, informed consent, misconduct, data fabrication and/or falsification, double publication and/or submission, and redundancy have been completely observed by the authors.

ABBREVIATIONS

A	Temperature
B	Time
AB	Interaction effect
AC	Activated carbon
AP	Adequate precision

APHA	American Public Health Association
ANOVA	Analysis of Variance
BET	Brunauer–Emmett–Teller
βo	Sum of a constant
C16H18N3S-Cl.3H2O	Methylene blue
CV	Coefficient of variation
CCD	Central composite design
COD	Chemical oxygen demand
CSA	Conventional steam activation
°C	Degree Celsius
df	Degree of freedom (df)
EFB	Empty fruit bunch
Fig.	Figure
FTIR	Fourier transform infrared (FTIR) spectroscopy
G	Grams
h	Hour
1/n	Heterogeneity factor related to Freundlich constant
K_2CO_3	potassium carbonate
KOH	potassium hydroxide
ktonnes	Kilo tonnes
KWh	Kilo Watt hour
Kg	Kilogram
L	Litres
L/mg	Langmuir constant
mg/L	Milligram per liter
mg/g	Milligram per gram
g/min	Gram per minute
g/L	Gram per litre
m^2/g	Metre square per gram
min	Minutes
MS	Mean squares
OPKS	Oil palm kernel shell
OPT	Oil palm trunks
OFAT	One factor at a time
OVAT	One variable at a time
p	Statistical significance of the difference
PAHs	Polycyclic aromatic hydrocarbons
PPF	Palm pressed fibres
RSM	Response surface methodology
RM	Ringgit
SEM	Scanning electron microscope
SS	Sum of squares
USD	United states dollar
Y	Predicted result

REFERENCES

Abdul Hamid, S.B.; Chowdhury, Z.Z.; Zain, S.M., (2014). Base catalytic approach: A promising technique for the activation of biochar for equilibrium sorption studies of copper, Cu(II) ions in single solute system, Materials. 7: 2815–2832 (**18 pages**).

Ahmad, R.; Mohd, M.A.; Nasulhah, I.N.; Ismail, K.K., (2019). Properties and thermal analysis of upgraded palm kernel shell and Mukah Balingian coal. Energy, 67: 538-547 **(10 pages).**

Ahmed, M.B.; Zhou, J.L.; Ngo, H.H.; Guo, W., (2016). Insight into biochar properties and its cost analysis. Biomass Bioenergy. 84: 76–86 **(11 pages).**

Amor, C.; Marchão, L.; Lucas, M.S.; Peres, J.A., (2019). Application of advanced oxidation processes for the treatment of recalcitrant agro-Industrial Wastewater: A Rev. Water 11(2): 205 **(31 pages).**

APHA, (2005). Standard methods for the examination of water and wastewater, American Public Health Association, 21st edition, Washington DC, USA.

Behera, S.K.; Meena, H.; Chakraborty, S. B.C.; Meikap, B.C., (2018). Application of response surface methodology (RSM) for optimization of leaching parameters for ash reduction from low-grade coal. Int. J. Min. Sci. Technol. 28: 621-629 (**9 pages**).

Chan, Y.H.; Quitain, A.T.; Yusup, S.; Uemura, Y.; Sasaki, M.; Kida, T., (2018). Liquefaction of palm kernel shell in sub- and supercritical water for bio-oil production. J. Energy Inst., 91: 721-732 **(12 pages).**

Chang, G.Z.; Miao, P.; Yan, X.; Wang, G.; Qing jie Guo, Q., (2018). Phenol preparation from catalytic pyrolysis of palm kernel shell at low temperatures. Biores. Technol., 253: 214 - 219 **(6 pages).**

Chen, X., (2015). Modeling of Experimental Adsorption Isotherm Data 2015, 6; 14-22 (**9 pages**).

Dai, Y.; Zhang, N.; Xing, C.; Cui, Q.; Sun, Q., (2019). The adsorption, regeneration and engineering applications of biochar for removal organic pollutants: A review. Chemosphere. 223: 12-27 **(16 pages).**

Daifullah, A. A. M.; Yakout, S. M.; Elreefy, S. A., (2007). Adsorption of fluoride in aqueous solutions using $KMnO_4$-modified activated carbon derived from steam pyrolysis of rice straw. J. Hazard. Mater. 147: 633–643 **(11 pages).**

Domeño, C.; Nerín, C., (2003). Fate of polyaromatic hydrocarbons in the pyrolysis of industrial waste oils. J. Anal. Appl. Pyrolysis, 67: 237–246 **(10 pages).**

Foo, K. Y.; Hameed, B. H., (2009). Utilization of biodiesel waste as a renewable resource for activated carbon: Application to environmental problems. Renew. Sustainable Energy Rev., 13:

2495–2504 **(10 pages).**

Foo, K.Y.; Hameed, B.H., (2012). Mesoporous activated carbon from wood sawdust by K_2CO_3 activation using microwave heating. Bioresour. Technol. 111: 425-432 **(8 pages).**

Goh, CS.; Tan, K.T.; Lee, K.T.; Bhatia, S., (2003) Bio-ethanol from lignocellulose: Status, perspectives and challenges in Malaysia. Bioresour. Technol. 101: 4834–4841 **(8 pages).**

Guo, J.; Lua, A.C., (2000). Preparation and characterization of adsorbents from oil palm fruit solid wastes, J. Oil Palm Res., 12: 64–70 (**7 pages**).

Guo, J.; Lua, A.C., (2002). Characterization of adsorbent prepared from oil-palm shell by CO2 activation for removal of gaseous pollutants, Mater. Lett. 55: 334–339 (**6 pages**).

Haeldermans, T.; Claesen, J.; Maggen, J.; Carleer, R.; Yperman, J.; Adriaensens, P.; Samyn, P.; Vandamme, D.; Cuypers, A.; Vanreppelen, K.; Schreurs, S., (2019). Microwave assisted pyrolysis of MDF: the influence of microwave power and microwave absorbers on the pyrolysis process and biochar characteristics. A comparison with conventional pyrolysis. J. Anal. Appl. Pyrol. 138: 218-230 **(13 pages).**

Jacyna, J.; Kordalewska, M.; Markuszewski, M.J., (2019) Design of Experiments in metabolomics-related studies: An overview. J. Pharm. Biomed. Anal. 164: 598–606 **(9 pages).**

Jamaluddin, M.A.; Ismail, K.; Mohd Ishak, M.A.; Ab Ghani, Z.; Abdullah, M. F.; Safian, M.; Idris, S.S.; Tahiruddin, S.; Yunus, M.F.M.; Mohd Hakimi, N.I.N., (2013). Microwave-assisted pyrolysis of palm kernel shell: Optimization using response surface methodology. Renew. Energy, 55: 357–365 (9 pages).

Junna, S.; He, F.; Pan, Y.; Zhang, Z., (2016). Effects of pyrolysis temperature and residence time on physicochemical properties of different biochar types. Acta Agric. Scand. B, 67: 1-11 **(11 pages).**

Karimifard, S.; Reza, M. M. A., (2018). Application of response surface methodology in physicochemical removal of dyes from wastewater: A critical review. Sci. Total Environ., 640-641: 772-797 **(26 pages).**

Lladó, J.; Solé-Sardans, M.; Lao-Luque, C.; Fuente, E.; Ruiz, B., (2016). Removal of pharmaceutical industry pollutants by coal-based activated carbons. Process Safe Environ. 104: 294–303 **(10 pages).**

Loh, S.K., (2017). The potential of the Malaysian oil palm biomass as a renewable energy source. Energy Convers. Manage 141: 285–298 **(14 pages).**

Makul, N.; Rattanadecho, P.; Agrawal, D.K., (2014). Applications of microwave energy in cement and concrete – A review. Renew. Sustainable Energy Rev., 37: 715–733 **(19 pages).**

Mazhari, M.P.; Hamadanian, M.; Mehipour, M.; Jabbari, V., (2018). Central composite design (CCD) optimized synthesis of $Fe3O4@SiO_2@AgCl/Ag/Ag_2S$ as a novel magnetic nano-photocatalyst for catalytic degradation of organic pollutants. J. Environ. Chem. Eng. 6: 7284 – 7293 **(10 pages).**

Nam, W.L.; Phang, X.Y.; Su, M.H.; Liew, R.K.; Lam, S.S., (2018). Production of bio-fertilizer from microwave vacuum pyrolysis of palm kernel shell for cultivation of Oyster mushroom (Pleurotus ostreatus). Sci. Total Environ., 624: 9-16 **(8 pages).**

Pathania, D.; Sharma, S.; Singh, P., (2017). Removal of methylene blue by adsorption onto activated carbon developed from Ficus carica bast. Arab. J. Chem., 10: S1445–S1451 **(7 pages).**

Rueda-Ordóñez, Y.J.; Arias-Hernández, C.J.; Manrique-Pinto, J.F.; Gauthier-Maradei, P.; Bizzo, W.A., (2019). Assessment of the thermal decomposition kinetics of empty fruit bunch, kernel shell and their blend. Biores. Technol. 292: 121923.

Rugayah, A.F.: Astimar, A.A.; Norzita, N., (2014). Preparation and Characterization of activated carbon frompalm kernel shell by physical activation with steam. J. Oil Palm Res., 26: 251-264 **(12 pages).**

Selvaraju, G.; Bakar, N.K.A., (2017). Production of a new industrially viable green-activated carbon from Artocarpus integer fruit processing waste and evaluation of its chemical, morphological and adsorption properties. J. Clean Prod., 141: 989–999 **(11 pages).**

Sumathi, S.; Bhatia, S.; Lee, K.T.; Mohamed, A.R., (2010). Selection of best impregnated palm shell activated carbon (PSAC) for simultaneous removal of SO_2 and NOx, J. Hazard. Mater. 176: 1093–1096 **(4 pages).**

Thiagarajan J.; Srividhya P.K.; Balasubramanian P., (2018). Thermal behavior and pyrolytic kinetics of palm kernel shells and Indian lignite coal at various blending ratios. Biores. Technol., 4: 88-95 **(8 pages).**

Xin-hui, D.; Srinivasakannan, C.; Jin-hui, P.; Li-bo, Z.; Zheng-yong, Z., (2011). Comparison of activated carbon prepared from Jatropha hull by conventional heating and microwave heating. Biomass Bioener., 35: 3920-3926 **(7 pages).**

Zainal, N.H.; Aziz, A.A.; Jalani, N.F.; Mamat, R., (2018). Carbonisation-activation system for the production of biochar and activated carbon from oil palm kernel shell. Malaysian Palm Oil Board Information series, ISSN 1511-7871.

Zhang, J.; Liu, J.; Liu, R., (2015). Effects of pyrolysis temperature and heating time on biochar obtained from the pyrolysis of straw and lignosulfonate. Bioresour. Technol., 176: 288-291 **(4 pages).**

Zhao, S.; Ta, N.; Wang, X., (2017). Effect of temperature on the structural and physicochemical properties of biochar with apple tree branches as feedstock material. Energies. 10: 1293 **(15 pages).**

AUTHOR (S) BIOSKETCHES

Affam, A.C., Ph.D., Department for Management of Science and Technology Development, Ton Duc Thang University, Ho Chi Minh City, Vietnam and Faculty of Environment and Labour Safety, Ton Duc Thang University, Ho Chi Minh City, Vietnam, Ton Duc Thang University, Ho Chi Minh City, Vietnam. Email: *augustine.chioma.affam@tdtu.edu.vn*

COPYRIGHTS

© 2020 The author(s). This is an open access article distributed under the terms of the Creative Commons Attribution (CC BY 4.0), which permits unrestricted use, distribution, and reproduction in any medium, as long as the original authors and source are cited. No permission is required from the authors or the publishers.

HOW TO CITE THIS ARTICLE

Affam, A.C., (2020). Conventional steam activation for conversion of oil palm kernel shell biomass into activated carbon via biochar product. Global J. Environ. Sci. Manage., 6(1): 15-30.

DOI: 10.22034/gjesm.2020.01.02

url: https://www.gjesm.net/article_36539.html